



Composite of Titanium Dioxide and Nickel Vanadate Application and Its Effect on Photocatalytic Degradation of Eosin yellow Dye

Yagnesh A. Vyas¹, Neetu Shorgar^{1*} and Mayank Mehta^{2*}

1. Department of Chemistry, Pacific Academy of Higher Education and Research, Udaipur, **INDIA**

2. Department of Chemistry, Gujarat University, Ahemdabad, **INDIA**

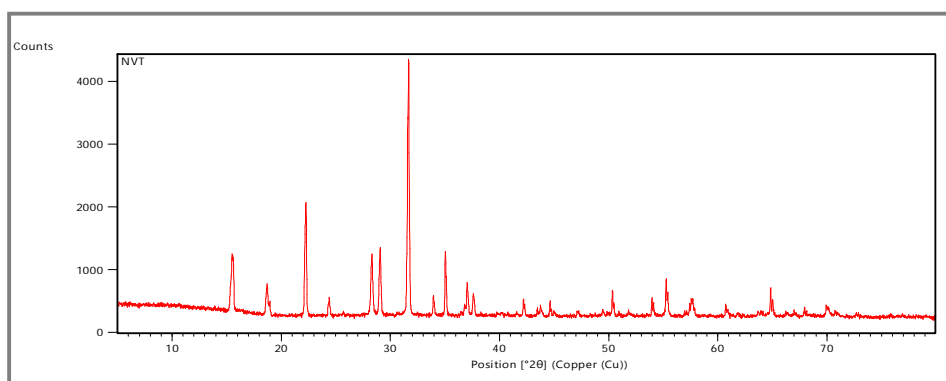
Emails: nshorgar@gmail.com, maku mehta@yahoo.com

Accepted on 8th May, 2023

ABSTRACT

Various photo catalysts have been used to separate various dyes from their aqueous solutions. As a photo catalyst for dye degradation, titanium oxide and nickel vanadate were combined. Numerous variables, such as the dye solution's pH, dye concentration, semiconductor amount, and light intensity, were studied for their impacts. The hydroxyl radical has been identified as an active oxidising species, which is a putative mechanism for the photocatalytic degradation of dye that has been the subject of significant study.

Graphical Abstract:



XRD of Nickle vanadate and Titanium Dioxide

Keywords: Nickel vanadate, Degradation, Eosin yellow. Photocatalysis.

INTRODUCTION

In order to make a graphene oxide/zinc oxide (GO/ZnO) nanocomposite, Durmus *et al.* [1] decorated thermally expanded and chemically oxidized graphite oxide nanosheets with zinc oxide (ZnO) nanoparticles made using a two-step sol-gel deposition procedure. They then used the composite as a successful photocatalyst for the degradation of the basic fuchsin (BF) dye. Zinc oxide (ZnO) nanoparticles made using a two-step sol-gel deposition technique are added to thermally expanded

and chemically oxidised graphite oxide Nano particles. In the modern world, there are many reasons of water pollution, which is a severe issue. Dyeing agents, which are used in the textile, paper, food, and other industries, are the principal cause of water pollution. Human activities, such as industrialization and agricultural practices, have significantly deteriorated and contaminated the environment, which has a detrimental effect on water bodies, which are necessary for life. TiO_2 , ZnO , WO_3 , and SnO_2 are a few metal oxide semiconductors that have been studied and employed as photo catalysts. TiO_2 is widely available, inexpensive, and chemically stable, making it the most effective photosensitizer. However, recent research has shown that ZnO may be used as a more efficient photocatalyst than TiO_2 [2, 3]. Sharma *et al.*, [4] used Bi_2O_3 and Bi_2S_3 to photocatalyze the breakdown of the blue B dye. Numerous parameters, such as pH, dye concentration, semiconductor amount, and light intensity, were observed and discussed. The progression of the photochemical oxidation was monitored spectrophotometrically. To determine the appropriate reaction conditions, experimental research was used. By using photochemistry, dye oxidation follows pseudo-first order kinetics. The final breakdown products were discussed, along with a potential photochemical oxidation procedure for dyes. The risk to the environment is significant as an outcome of the extensive use of organic dyes in chemical waste from the paper, textile, and garment sectors [5]. A significant portion (20%) of the dyes used in the textile industry each year, including Rhodamine B, Victoria blue, Rose Bengal, Indigo Red, Carmine, Red 120, Eriochrome, Methylene Blue (MB), Black-T (EBT), and Thymol blue, are lost during the synthesis and processing processes and end up in wastewater, according to a number of studies [6-10]. Several factors affect the entire photo degradation process, from the adsorption of dye molecules on the photo catalyst surface to the breakdown of dye molecules by acute radicals. Processing factors like the starting dye quantity, solution pH, and irradiation intensity [11-18]. The colour and characteristics of dye molecules are determined by their chemical structure. . Over 50% of all industrial dyes used are azo dyes, which are thought to contain the largest group of colorants among the major dye classifications. Dyes [19] based to their chemical composition, dyes are divided into cationic and anionic dyes. Rhodamine B (RhB), crystal violet (CV), rhodamine 6G (Rh6G), safranin O (SO), and MB are examples of cationic dyes that include chemical groups that can separate into positively charged ions studied by G. Ramesha [20].

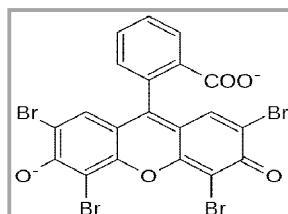


Figure 1. Structure of Eosin Yellow.

MATERIALS AND METHODS

Synthesis of Nickle Vanadate: In 400 mL of water that had been distilled, 4.68 g of nickel sulphate (NiSO_4) was dissolved. The formal term for it is solution A. Solution B was made by dissolving 21.02 g of ammonium metavanadate (NH_4VO_3) in 400 mL of distilled water. For 4 h, solutions A and B were aggressively magnetically swirled together. The resulting slurry was then transferred to a new beaker and heated for 20 min at 180°C in order to evaporate the water from the substance. After being gradually brought to room temperature, the precipitate was repeatedly washed with distilled water, and it was then dried for 5–6 h to yield greenish yellow nickel vanadate powder.

Solution Preparation: Double-distilled water was used to make all of the solutions. In a 1:1 ratio, nickel vanadate was mixed with titanium dioxide Composite characterization: EDX Analysis: Energy-dispersive X-ray spectroscopy (EDS) detects X-rays released from a sample during electron beam bombardment to analyze the constituent composition. Table 1 summarizes the findings, and figure 2 depicts them.

Characterization of composite: EDX Analysis: When a sample is bombarded by an electron beam to determine its elemental composition, energy-dispersive X-ray spectroscopy (EDS) looks for X-rays that are released from the sample. Table 1 presents the findings, and figure 2 displays the findings.

Element [wt.%]	Series [wt.%]	C norm. [wt.%]	C Atom. [wt.%]
Vanadium	K-series	60.47	52.21
Titanium	K-series	30.80	28.30
Oxygen	K-series	6.43	17.67
Aluminium	K-series	0.10	0.16
Nickel	K-series	2.20	1.65

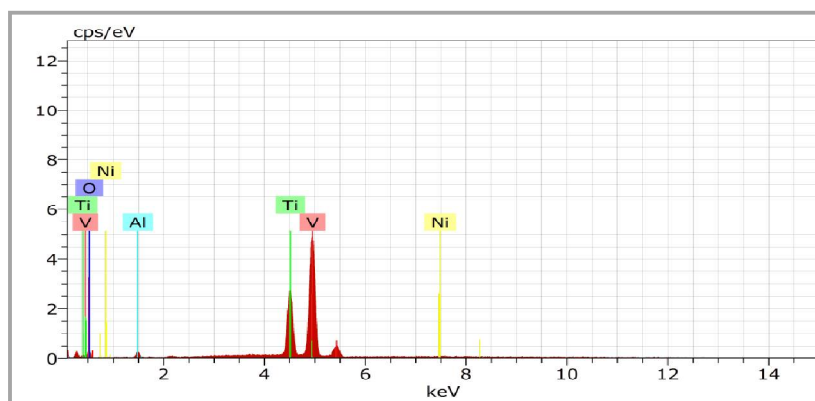


Figure 2. EDS of Nickle vanadate and Titanium Dioxide.

RESULTS AND DISCUSSION

XRD Analysis: X-rays are electromagnetic radiation waves, whereas crystals are regular collections of atoms. Crystal atoms primarily interact with their electrons to deflect incoming X-rays. The dispersion of the electron is a component of the process known as elastic scattering. A regular array of spherical waves results from a regular array of scatterers. These waves interact destructively in the majority of directions, but in the following few, according to Bragg's law, they add: A non-destructive method known as X-ray diffraction analysis (XRD) may give accurate details on a material's crystallographic structure, chemical makeup, and physical characteristics. It appears with a start position of 5.0084 and an end position of 79.9784, respectively, the minimum step sizes for 2Theta and Omega are 0.001 and 0.001, respectively. Size of Divergence Slit [°] 0.4354, and the powder XRD are displayed in figure 3.

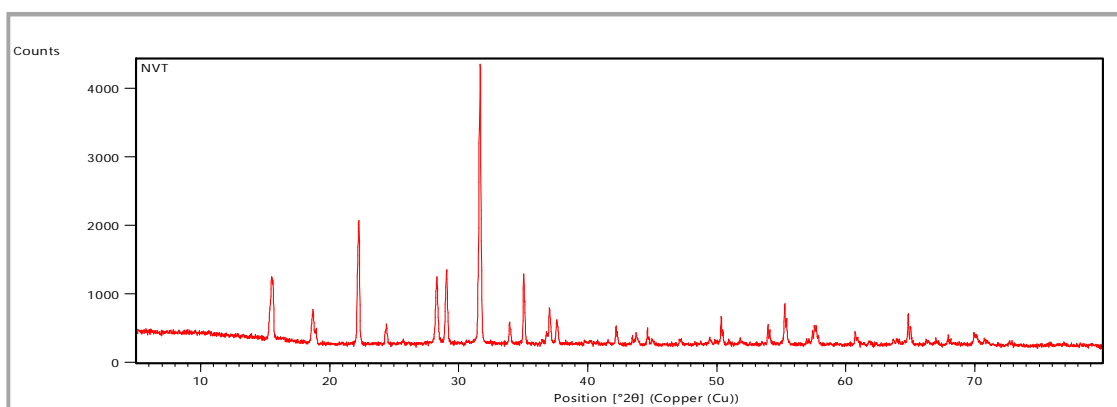


Figure 3. XRD of Nickle vanadate and Titanium Dioxide.

Photocatalytic Process: Eosin yellow was dissolved in 100.0 mL of twice-distilled water at a rate of 0.06912 g g^{-1} , yielding a dye solution concentration of $10 \times 10^{-3} \text{ M}$. It was once used as a stock medicine. This stock solution was further diluted. The absorbance of eosin yellow solution at $\lambda_{\text{max}} = 510 \text{ nm}$ was calculated using a spectrophotometer. The dye solution was divided equally among four beakers. The first beaker, which contained the Eosin yellow solution, was kept in the shadows. The second beaker's Eosin yellow solution was lit. The third beaker was kept in the dark and contained 0.10 g of nickel vanadate and titanium dioxide composite as well as Eosin Yellow Solution. The fourth beaker was lighted, which contained 0.10 g of vanadate and an Eosin yellow solution. After three to four hours, the absorbance of each beaker's solution was measured using a spectrophotometer. The absorbance of the solutions in the first three beakers practically remained constant, while the absorbance of the solution in the fourth beaker fell from its initial value, it was found. This result makes it clear that both light and the semiconductor nickel vanadate and titanium dioxide composite are necessary for this reaction to happen. As a result, this reaction is photocatalytic in nature. Double-distilled water contains a solution of $1.30 \times 10^{-5} \text{ M}$ Eosin yellow was produced, and 0.10 g of nickel vanadate and titanium dioxide composite was added. The pH of the reaction mixture was raised to 9.5 and then illuminated with a 200 W tungsten lamp at 50.0 mWcm^{-2} . The absorbance of Eosin yellow solution decreased with longer exposure times. The photocatalytic degradation of eosin yellow follows pseudo first order kinetics, as shown by a linear plot of $1 + \log A$ against time with

$$k = 2.303 \text{ slope... (1)}$$

Table 1. A Typical Run

pH = 9.0 Eosin Yellow = $1.30 \times 10^{-5} \text{ M}$
 Nickel Vanadate and TiO_2 composite = 0.10 Light intensity = 50.0 mWcm^{-2}

Time (min)	Absorbance A	1+log OD
0.0	1.202	1.0799
10.0	1.152	1.0614
20.0	1.102	1.0421
30.0	1.056	1.0236
40.0	1.002	1.0008
50.0	0.966	0.9849
60.0	0.913	0.9604
70.0	0.881	0.9449
80.0	0.852	0.9304
90.0	0.819	0.9132
100.0	0.796	0.9009

Rate Constant = $6.24 \times 10^{-5} \text{ Sec}^{-1}$

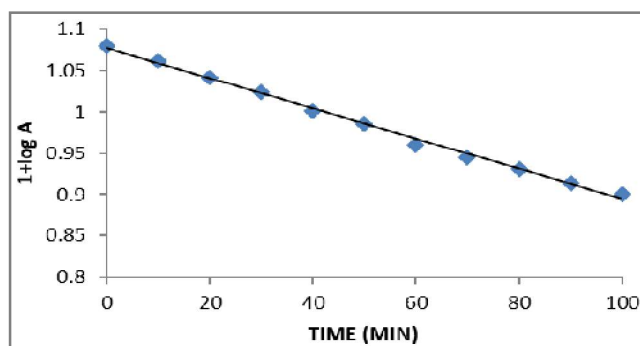


Figure 4. A Typical Run.

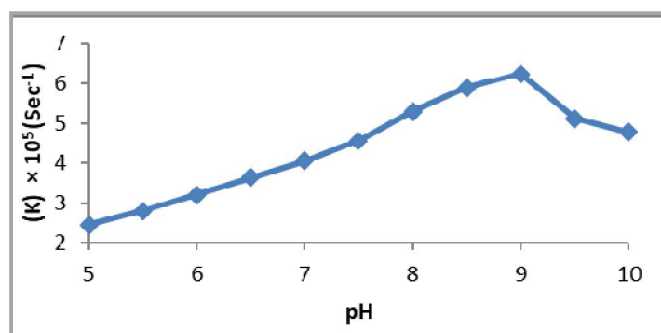
The Impact of pH: The pH of the solution is possibly a factor in eosin yellow degradation. The effect of pH on the rate of Eosin yellow degradation was investigated in the pH range of 5.0-10.5. Results are presented graphically in Figure 5 and are summarized in table 2.

Table 2. Effect of pH

Eosin yellow= 1.30×10^{-5} M Nickel Vanadate and TiO_2 composite= 0.10 g
Light intensity = 50.0 mWcm^{-2}

pH	Rate Constant (K) $\times 10^5 (\text{Sec}^{-1})$
5.0	2.44
5.5	2.79
6.0	3.20
6.5	3.64
7.0	4.05
7.5	4.56
8.0	5.30
8.5	5.89
9.0	6.24
9.5	5.12
10.0	4.79

The rate of photocatalytic degradation of eosin yellow has been seen to increase with pH, peaking at 9.0 pH. As pH was increased further, the rate of the reaction slowed. The fact that the rate of photocatalytic degradation increases with pH may be used to explain this trend because there is a larger chance that oxygen anion radicals (O^{2-}), which are created when oxygen molecules combine with semiconductor electrons (e^-), will take place. Photo catalysis causes the dye to break down more quickly. Because of the absorption of OH^- ions, the anionic form of Eosin yellow will reject the negatively charged semiconductor surface, which may be the reason why the rate of the dye's photocatalytic degradation reduced beyond pH 9.0.

**Figure 5.** Effect of pH.

The Impact of the Dye Concentration: To investigate the effects of dye concentration, eosin yellow was used in a range of concentrations. The results are represented visually in figure 6 and listed in table 3.

Table 3. Effect of Eosin Yellow Concentration

pH = 9.0 Nickel Vanadate and TiO_2 composite= 0.10 g
Light intensity = 50.0 mWcm^{-2}

[Eosin Yellow] $\times 10^5 \text{ M}$	Rate Constant (K) $\times 10^5 (\text{Sec}^{-1})$
0.9	4.56
1.0	4.92
1.1	5.48
1.2	5.81
1.3	6.24
1.4	5.62
1.5	5.02
1.6	4.72
1.7	4.60
1.8	4.43

The rate of dye degradation by photocatalysis rises when Eosin yellow concentration is raised to 1.30×10^{-5} M. It might be because more dye molecules were available for excitation and energy transfer as dye concentration rose, leading to an increase in the rate of dye degradation. In order to avoid the dye from serving as an internal filter and preventing the necessary light intensity from reaching the surface of the semiconductor at the bottom of the reaction vessel, a drop in rate was seen when dye concentration was elevated over 1.30×10^{-5} M.

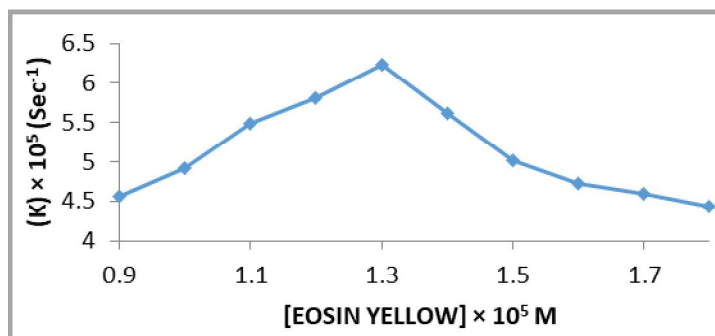


Figure 6. Effect of Dye Concentration.

Effect of semiconductor: Performance Since it is expected that the amount of semiconductor will also have an effect on the degradation of dye, different amounts of photo catalyst were used. Figure 7 presents the findings graphically and summarises the information from table 4.

Table 4. Effect of Amount of Nickel Vanadate and Titanium Dioxide Composite

pH = 9.0 [Eosin Yellow] = 1.30×10^{-5} M
Light intensity = 50.0 mWcm⁻²

Nickel Vanadate and TiO ₂ (g)	Rate Constant (K) × 10 ⁵ (Sec ⁻¹)
0.02	2.19
0.03	2.42
0.04	3.21
0.05	3.82
0.06	4.12
0.07	4.47
0.08	5.39
0.09	5.84
0.10	6.24
0.11	6.01
0.12	5.70
0.13	5.61
0.14	5.52

It was discovered that the rate of reaction increases as the amount of semiconductor nickel vanadate and titanium dioxide composite increases. The rate of degradation was accelerated by the 0.10 g photocatalyst concentration. Above 0.10 g, the rate constant was almost constant. This can be the case because when semiconductor was used, the exposed semiconductor surface area increased. However, the semiconductor layer only gets thicker and the exposed surface area does not occur once the amount of semiconductor exceeds this limiting threshold (0.10 g). This was confirmed using reaction containers of various sizes. The saturation point rises upward for bigger vessels whereas smaller vessels show the opposite tendency.

Light Intensity's Effect: The distance between the light source and the exposed photocatalyst surface area was changed to examine the impact of light intensity on the photocatalytic degradation of Eosin yellow. The results are described in table 5, and figure 8 presents the data graphically.

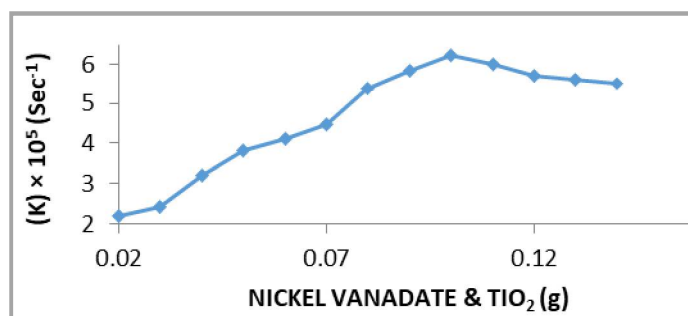


Figure 7. Effect of Ammount of Nickel Vanadate and TiO₂(g).

Table 5. Effect of Light Intensity

pH = 9.0 [Eosin Yellow] = 1.30×10^{-5} M
 Nickel Vanadate and TiO₂ composite= 0.10 g

Light Intensity mWcm ⁻²	Rate Constant (K) × 10 ⁵ (Sec ⁻¹)
20.0	3.12
30.0	4.01
40.0	5.13
50.0	6.24
60.0	6.02
70.0	5.89

The statistics reveal that degradation accelerated as light intensity climbed since any increase in light intensity will increase the number of photons striking per unit area of semiconductor powder per unit time. However, when the intensity was increased over 50.0 mWcm⁻², there was a slight decrease in the rate. This could happen as a result of different negative impacts.

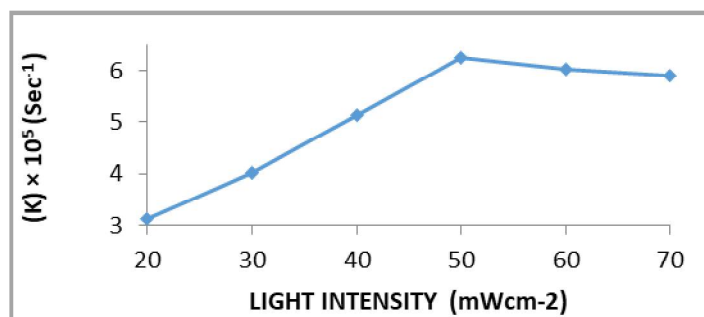
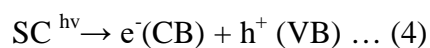


Figure 8. Effect of Light Intensity

Mechanism: The following mechanism for the photocatalytic degradation of the dye Eosin yellow is suggested by these data:





When eosin yellow (EY) dye absorbs photons of the right wavelength, it creates its initial excited singlet state. The dye then enters the triplet state as a result of intersystem crossover (ISC). On the other hand, an electron is excited from the valence band to the conduction band in the semiconducting nickel vanadate and titanium dioxide composite. This electron will be captured by the oxygen molecule (dissolved oxygen), forming the superoxide anion radical (O⁻). This anion radical will change the Eosin Yellow dye into its leuco form, which may eventually degrade to products. As an oxidising species, the OH radical does not actively contribute to this degradation. Furthermore, the rate of degradation was unaffected by the addition of a hydroxyl radical scavenger, indicating that reduction rather than oxidation is the mechanism underlying this degradation of 2-propanol.

APPLICATION

This study is very successful for eliminating toxins from industrial wastewater from firms such as pigment manufacturing, health care, and papermaking, among others.

CONCLUSION

A titanium dioxide and nickel vanadate photo catalyst composite was used to decompose the eosin yellow dye. The experimental results showed that the photocatalytic degradation efficiency of eosin yellow dye was affected by pH, dye solution concentration, semiconductor amount, and light intensity. It is possible to investigate how various different contaminants degrade in relation to how the photo catalyst is used.

REFERENCES

- [1]. Z. Durmus, B. Z. A. Kurt, Durmus, Synthesis and characterization of graphene oxide/zinc oxide (GO/ZnO) nanocomposite and its utilization for photocatalytic degradation of basic fuchsin dye, *Chemistry Select*, **2019**, 4(1), 271-278
- [2]. M. Ahmad, E. Ahmad, Y.W. Zhang, N. R. Khalid, J. F. Xu, M. Ullah, Z. L. Hong, Preparation of Highly Efficient Al-Doped ZnO Photocatalyst by Combustion Synthesis, *Current Applied Physics*, **2013**, 13, 697-704. <http://dx.doi.org/10.1016/j.cap.2012.11.008>
- [3]. Z. H. Xiao, W. Hu, X. B. Zhou, X.W. Zheng, Fabrication of Erbium-Doped Spherical Like ZnO Hierarchical Nanostructures with Enhanced Visible Light-Driven Photocatalytic Activity. *Materials Letters*, **2013**, 91, 1-4.
- [4]. D. K. Sharma, A. Bansal, R. Ameta and H. S. Sharma, Photodegradation of Azure B with the Help of Bismuth Oxide and Bismuth Sulphide used as Photocatalyst: A Comparative Study, *Int. J. Chem. Tech. Res.*, **2013**, 5(2), 578-584.
- [5]. Y.-H. Chiu, T.-F.M. Chang, C.-Y. Chen, M. Sone, Y.-J. Hsu, *Catalysts*, **2019**, 9(5), 430.
- [6]. I. K. Konstantinou, T. A. Albanis, *Applied Catal. B: Environ.*, **2004**, 49 (1), 1.
- [7]. F. Deng, L. Min, X. Luo, S. Wu, S. Luo, *Nanoscale*, **2013**, 5(18), 8703.
- [8]. S. Xu, Y. Zhu, L. Jiang, Y. Dan, *Water Air Soil Pollut.*, **2010**, 213(1-4), 151.
- [9]. D. Wang, Y. Wang, X. Li, Q. Luo, J. An, J. Yue, *Catal. Commun.*, **2008**, 9(6), 1162.
- [10]. A. Kumar, G. Pandey, *Mater. Sci. Eng. Int. J.*, **2017**, 1(3), 1.
- [11]. T. Shahwan, *et al.*, *Chem. Eng. J.*, **2011**, 172 (1), 258.
- [12]. B. Neppolian, H. Choi, S. Sakthivel, B. Arabindoo, V. Murugesan, J. Hazard. *Mater.*, **2002**, 89 (2-3), 303.
- [13]. Z. Shams-Ghahfarokhi, A. Nezamzadeh-Ejhi, *Mater. Sci. Semicond. Process*, **2015**, 39, 265.

- [14]. C. Guillard, H. Lachheb, A. Houas, M. Ksibi, E. Elaloui, J.-M. Herrmann, *J. Photochem. Photobiol., A: Chem.*, **2003**, 158 (1), 27.
- [15]. F. Akbal, *Environ. Prog.*, **2005**, 24 (3), 317.
- [16]. M. Ikram, et al., *RSC Adv.*, **2020**, 10 (50), 30007
- [17]. M. Ikram, et al., *RSC Adv.*, **2020**, 10 (41), 24215
- [18]. Y.-H. Chiu, T.-F.M. Chang, C.-Y. Chen, M. Sone, Y.-J. Hsu, *Catalysts.*, **2019**, 9 (5), 430
- [19]. A. Ajmal, I. Majeed, R.N. Malik, H. Idriss, M.A. Nadeem, *RSC Adv.*, **2014**, 4 (70), 37003.
- [20]. G. Ramesha, A.V. Kumara, H. Muralidhara, S. Sampath, *J. Colloid Interface Sci.*, 2011, 361 (1), 270.